Protonation Studies of Modified Adenine and Adenine Nucleotides by Theoretical Calculations and ^{15}N NMR

Dan T. Major, Avital Laxer, and Bilha Fischer*

Department of Chemistry, Gonda-Goldschmied Medical Research Center, Bar-Ilan University, Ramat-Gan 52900, Israel

bfischer@mail.biu.ac.il

Received July 25, 2001

The acid/base character of nucleobases affects phenomena such as self-association, interaction with metal ions, molecular recognition by proteins, and nucleic acid base-pairing. Therefore, the investigation of proton-transfer equilibria of natural and synthetic nucleos(t)ides is of great importance to obtain a deeper understanding of these phenomena. For this purpose, a set of ATP prototypes was investigated using ^{15}N NMR spectroscopy, and the corresponding adenine bases were investigated by theoretical calculations. ^{15}N NMR measurements provided not only acidity constants but also information on the protonation site(s) on the adenine ring and regarding the ratio of the singly protonated species in equilibrium. Substituents of different nature and position on the adenine ring did not change the preferred protonation site, which remained N1. However, for 2-thioether-ATP derivatives a mixed population of N1 and N7 singly protonated species was observed. Reduction of basicity of 0.4−1 pK_a units relative to ATP was also observed for all evaluated ATP derivatives, except for 2-Cl-ATP, for which K_a was ca. 10,000-fold lower. To explain the substitution-dependent variations in the experimental pK_a values of the ATP analogues, gas-phase proton affinities (PA), $\Delta\Delta G^{hyd}$, and pK_a values of the corresponding adenine bases were calculated using quantum mechanical methods. The computed PA and $\Delta\Delta G^{hyd}$ values successfully explained the experimental pK_a values. A computational procedure for the prediction of accurate pK_a values was developed using density functional theory and polarizable continuum model calculations. In this procedure, we developed a set of parameters for the polarizable continuum model that was fitted to reproduce experimental pK_a values of nitrogen heterocycles. This method is proposed for the prediction of pK_a values and protonation site(s) of purine analogues that have not been synthesized or analyzed.

Introduction

Natural and synthetic adenine nucleosides and nucleotides comprise a class of biologically important molecules. Intracellular ATP plays a fundamental role in energy metabolism, nucleic acid synthesis, pump activities, and enzyme regulation. Additionally, there is now widespread evidence that extracellular adenine nucleos(t)ides mediate signals via membrane-associated adenosine and ATP receptors.[1]

An important factor in the functionality of adenine nucleos(t)ides is their ability to participate in acid−base equilibria. The acidity of natural and synthetic adenine nucleos(t)ides affects phenomena such as self-association; interaction with metal ions; interaction with receptors and enzymes; and base-pairing in nucleic acids, which influences their structure, stability, and function.[2]

There are several possible ionizable sites in adenine nucleos(t)ides: the phosphate, base, or sugar moieties. The most basic position on the adenine ring is N1.[3,4] Protonation occurs on the pyrimidine ring of the purine base even though pyrimidine itself is a weaker base than imidazole. This protonation is due to the imidazole NH nitrogen, which is strongly electron-donating to the pyrimidine ring.[4b] Furthermore, the exocyclic N^6-amine in adenine is an efficient electron donor that increases electron density on N1, as reflected by the 100-fold increase in basicity of adenine vs purine.[5] On the other hand, the affinity of N7 in adenine nucleotides for proton is very low.[6] For instance, the pK_a of N7 of 5′-AMP is

* To whom correspondence should be addressed: Fax: 972-3-5351250. Tel: 972-3-5318303.

(1) (a) Fredholm, B. B.; Arslan, G.; Halldner, L.; Kull, B.; Schulte, G.; Wasserman, W. *Naunyn−Schmiedeberg's Arch. Pharmacol.* **2000**, *362*, 364−374. (b) Bhagwat, S. S.; Williams, M. *Eur. J. Med. Chem.* **1997**, *32*, 183−193. (c) Fischer, B. *Expert Opin. Ther. Patents* **1999**, *9*, 385−399.

(2) (a) Legault, P.; Pardi, A. *J. Am. Chem. Soc.* **1997**, *119*, 6621−6628. (b) Gforer, A.; Schnetter, M.; Wolfrum, J.; Greulich, K. D. *Ber. Bunsen-Ges. Phys. Chem.* **1989**, *93*, 300−304. (c) Cali, R.; Musumeci, S.; Rigano, C.; Sammartano, S. *Inorg. Chim. Acta* **1981**, *56*, L11−L13.

(3) (a) Saenger, W. *Principles of Nucleic Acid Structure*; Springer-Verlag: New York, 1984; pp 107−110. (b) Sysoeva, S. G.; Utyanskaya, E. Z.; Vinnik, M. I. *Izv. Akad. Nauk, Ser. Khim.* **1983**, *7*, 1505−1511. (c) Raszka, M. *Biochemistry* **1974**, *13*, 4616−4622. (d) Tribolet, R.; Sigel, H. *Eur. J. Biochem.* **1987**, *163*, 353−363.

(4) (a) Sigel, H.; Scheller, K. H.; Milburn, R. M. *Inorg. Chem.* **1984**, *23*, 1933. (b) Lister, J. H. Fused Pyrimidines; Interscience: New York, 1971; p. 444. (c) Buchner, P.; Maurer, W.; Ruterjans, H. *J. Magn. Reson.* **1978**, *29*, 45−63.

(5) Gonella, N. C.; Roberts, J. D. *J. Am. Chem. Soc.* **1982**, *104*, 3162−3164.

(6) Utyanskaya, E. Z.; Lezina, V. P.; Stepanyants, A. U. *Izv. Akad. Nauk, ser. Khim.* **1986**, *12*, 2691−2696.

10.1021/jo0107554 CCC: $22.00
Published on Web 01/10/2002

−1.6; this adenine nitrogen is protonated only after complete protonation of N1.[7]

A multitude of modified adenines and adenine nucleos(t)ides have been synthesized as inhibitors for enzymes or as agonists/antagonists to target receptors.[1c] Modifications, such as substitution of the adenine ring with electron-donating (ED) or electron-withdrawing (EW) substituents, can substantially alter the electronic properties of the purine ring. Such a change in the charge distribution of the nucleobase is expected to influence the acid−base properties of the molecule and possibly change the site of protonation. Therefore, a systematic evaluation of the basicity of substituted adenines and adenine nucleos(t)ides is important and may shed light on the chemical and biochemical properties of these nucleos(t)ides.

In general, ionization constants are directly measured by pH titration monitored by a variety of spectroscopic techniques. Acidity constants for nucleos(t)ides have been obtained by ^{1}H NMR,[8] IR,[9] potentiometric titrations,[10] etc. However, most of these methods do not provide information on the site of protonation in the nucleobase (e.g., N1 or N7). This lack of information is a severe drawback, especially since the preferred site of protonation may be altered upon substitution on the nucleobase and several singly protonated species may coexist.

An alternative spectroscopic method is ^{15}N NMR, which allows unambiguous determination of the protonation site. This determination is due to the direct measurement of the nitrogens undergoing protonation and the great sensitivity of this spectroscopic method to protonation. For example, protonation of the N1-position in ATP causes an upfield shift of ca. 70 ppm.[11]

Indeed, ^{15}N NMR has been utilized for studies of protonation in nucleosides, nucleotides, nucleic acids, and protein-bound nucleotides.[11a,12] However, as a result of the limited solubility of nucleobases and nucleosides in water, various reports describe their protonation in DMSO solutions, with trifluoroacetic acid.[13] Therefore, no pK_a values are provided based on ^{15}N NMR.[11a,13] Nevertheless, ^{15}N NMR may be a suitable tool for pK_a determination for nucleotides, which are highly water soluble.

Although the experimental determination of pK_a values is usually the most reliable option, theoretical calculations can be used to supplement and rationalize experimental data. Sometimes, experimental determination of pK_a values of compounds may be complex or even impossible, as a result of either a very high or very low acidity, or because of low solubility in water. Therefore, a theoretical approach serves as a possible solution for such cases. Moreover, a theoretical approach enables the prediction of pK_a values of derivatives that have not been synthesized.

Scheme 1

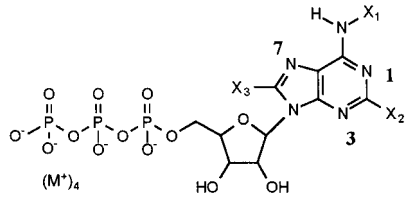

1 X_1=X_2=X_3=H
2 X_1=X_3=H, X_2=SCH_3
3 X_1=X_3=H, X_2=$SCH_2C(CH_3)_3$
4 X_1=CH_3, X_2=X_3=H
5 X_1=X_3=H, X_2=Cl
6 X_1=X_2=H, X_3=Br

In this paper, we report pK_a values and protonation sites of several prototypic ATP derivatives estimated by ^{15}N NMR. In addition, we propose a theoretical method for the prediction of basicity and protonation sites of adenine bases based on Density Functional Theory (DFT) calculations. The effects of ED and EW substituents on the pK_a values of adenine derivatives are discussed in light of the present results.

Results

Selection of ATP Derivatives Prototypes. The pK_a values and protonation sites of synthetic ATP prototypes used in our previous biochemical studies[14,15] were determined by ^{15}N NMR.

The set of the investigated adenine-modified ATP derivatives is shown in Scheme 1. The structural changes included substituents of different electronic nature (ED or EW) and of different volume substituted at different positions on the adenine ring (C2, N^6, C8).

Synthesis. Compounds **2** and **3** were prepared from 2-thiol-adenosine[16] by selective S-alkylation of the thiolate salt of **7** with alkyl bromide/iodide and subsequent one-pot 5′-triphosphorylation[14c] (Scheme 2). 2-Chloroadenosine, **11**, was prepared in 73% yield from 2,6-dichloro-9β-(2′,3′,5′-tri-*O*-acetyl)-D-ribofuranosylpurine, **10**,[17] upon heating to 100° C for 24 h in a sealed ampule containing 2 M NH_3/EtOH (Scheme 3). This method is superior to the common preparation of 2-chloro-adenosine.[18] Only NH_3/EtOH is useful in our procedure and not NH_3/MeOH, because in the latter case 2-chloro-6-meth-

(7) Martin, R. B. *Acc. Chem. Res.* **1985**, *18*, 32−38.
(8) Wang, P.; Izatt, R. M.; Oscarson, J. L.; Gillespie, S. E. *J. Phys. Chem.* **1996**, *100*, 9556−9560.
(9) Hofmann, K. P.; Zundel, G. *Z. Naturforsch., C: Biosci.* **1974**, *29*, 19−28.
(10) Tribolet, R.; Malini-Balakrishnan, R.; Sigel, H. *J. Chem. Soc., Dalton Trans.* **1985**, 2291−2303.
(11) (a) Markowski, V.; Sullivan, G. R.; Roberts, J. D. *J. Am. Chem. Soc.* **1977**, *99*, 714−718. (b) Buchanan, G. W. *Tetrahedron* **1989**, *45*, 581−604.
(12) (a) Hovinen, J.; Glemarec, C.; Sandström, A.; Sund, C.; Chattopadhyaya, J. *Tetrahedron* **1991**, *47*, 4693−4708. (b) Gonella, N. C.; Nakanishi, H.; Holtwick, J. B.; Horowitz, D. S.; Kanamori, K.; Leonard, N. J.; Roberts, J. D. *J. Am. Chem. Soc.* **1983**, *105*, 2050−2055. (c) Rhee, Y.; Wang, C.; Gaffney, B. L.; Roger, R. A. *J. Am. Chem. Soc.* **1993**, *115*, 8742−8746. (d) Drohat, A. C.; Stivers, J. T. *J. Am. Chem. Soc.* **2000**, *122*, 1840−1841.
(13) Buchanan, G. W.; Bell, M. J. *Can. J. Chem.* **1983**, 2445−2448.
(14) (a) Fischer, B.; Boyer, J. L.; Hoyle, C.; Ziganshin, A.; Ralevic, V.; Knight, G.; Brizzolara, A.; Zimmet, J.; Burnstock, G.; Harden, T. K.; Jacobson, K. A. *J. Med. Chem.* **1993**, *36*, 3937−3946. (b) Burnstock, G.; Fischer, B.; Hoyle, C. H. V.; Maillard, M.; Ziganshin, A. U.; Brizzolara, A. L.; von Isakovics, A. K.; Boyer, J. L.; Harden, T. K.; Jacobson, K. A. *Drug Dev. Res.* **1994**, *31*, 206−219. (c) Halbfinger, E.; Major, D. T.; Ritzmann, M.; Ubl, J.; Reiser, G.; Boyer, J. L.; Harden, K. T.; Fischer, B. *J. Med. Chem.* **1999**, *42*, 5325−5337 (d) Major, D. T.; Halbfinger, E.; Fischer, B. *J. Med. Chem.* **1999**, *42*, 5338−5347.
(15) Gendron, F.-P.; Halbfinger, E.; Fischer, B.; Duval, M.; D'Orleans-Juste, P.; Beaudoin, A. R. *J. Med. Chem.* **2000**, *43*, 2239−2247.
(16) (a) Kikugawa, K.; Suehiro, H.; Ichino, M. *J. Med. Chem.* **1973**, *16*, 1381−1388. (b) Kikugawa, K.; Suehiro, H.; Yanase, R.; Aoki, A. *Chem. Pharm. Bull.* **1977**, *25*, 1959−1969 and references therein.
(17) (a) Robins, M. J.; Uznanski, B. *Can. J. Chem.* **1981**, *59*, 2601−2606. (b) Nair, V.; Richardson, S. G. *Synthesis* **1982**, 670−672.
(18) Montgomery, J. A.; Hewson, K. *J. Heterocycl. Chem.* **1964**, *1*, 213−214.

Scheme 2[a]

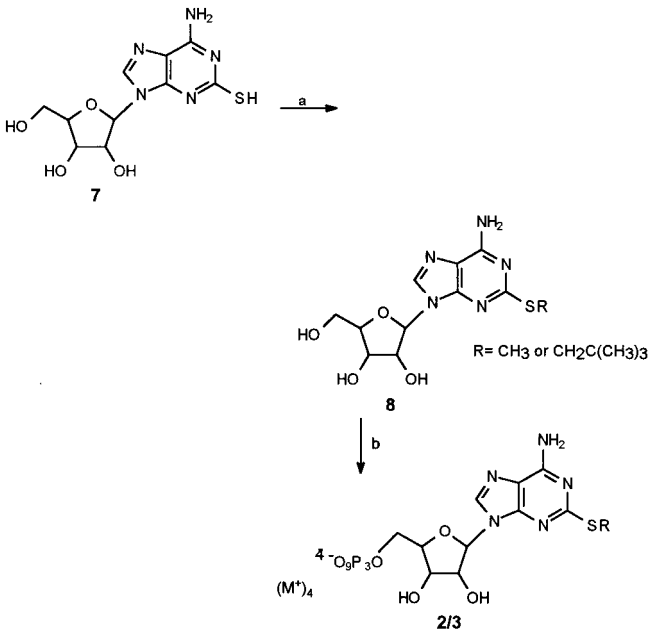

[a] Conditions: (a) (1) NaOH, isolation, (2) CH_3I/DMF for **1** or (1) 0.25 M NaOH/MeOH, isolation, (2) $BrCH_2C(CH_3)_3$/DMF for **2**; (b) (1) $POCl_3$, $PO(OCH_3)_3$, (2) $(Bu_3NH^+)_2H_2P_2O_7^{2-}$, (3) hydrolysis.

Scheme 3[a]

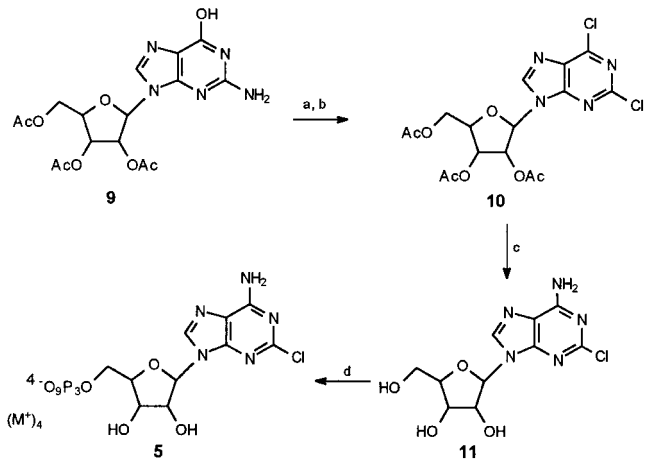

[a] Conditions: (a) $POCl_3$, CH_3CN; (b) $(CH_3)_2CHCH_2CH_2ONO$, CCl_4; (c) NH_3/EtOH; (d) (1) $POCl_3$, $PO(OCH_3)_3$, (2) $(Bu_3NH^+)_2H_2P_2O_7^{2-}$, (3) hydrolysis.

oxy-purine riboside was also obtained in approximately 60% yield. 2-Chloro-adenosine was then 5′-triphosphorylated to give derivative **5**.

^{15}N NMR Measurements. ^{15}N NMR spectra of trisodium salts of ATP derivatives **1**−**6** were measured at natural abundance in H_2O solutions at pH 5.2−5.4. The results are summarized in Table 1.

A major parameter determining the ^{15}N chemical shift of a heterocyclic nitrogen is its π-electron density.[19] For instance, N9 in the purine ring system has a high π-electron density since it provides two electrons to the delocalized π-orbital system, whereas N1, N3, and N7 have a lower π-electron density since they provide only one electron. Therefore, ^{15}N chemical shift of N9 is shifted 40−60 ppm upfield relative to N1, N3, and N7 (Table 1). Changes of nitrogens' chemical shifts in substituted adenines, described below, are discussed in the light of changes in π-electron density due to substitution.

The electron-withdrawing effect of chlorine at the C2 position in 2-Cl-ATP is clearly observed by the downfield shift of N1 as compared to the shift of N1 of ATP ($\Delta\delta$ +6.5 ppm), Table 1, and also in the chemical shift of the exocyclic amine in 2-Cl-ATP ($\Delta\delta$ +5 ppm). These results are consistent with our previous theoretical findings on electron density on 2-Cl-adenine nitrogens.[14d] The deshielding effect of Br substituent in 8-Br-ATP is more pronounced at the endocyclic nitrogens, especially on N7 ($\Delta\delta$ +7.6 ppm). N9, on the other hand, undergoes an upfield shift ($\Delta\delta$ −3.4 ppm). 2-Alkylthio- and N^6-methyl substitutions have only a minor effect on the exo- and endocyclic nitrogens, except for N3 where an upfield shift ($\Delta\delta$ −5.4 and −4.4 ppm, respectively) is observed. This finding indicates higher electron density due to mesomeric contributions. In all of the ATP derivatives, with the exception of 2-MeS-ATP, N1 is deshielded relative to N1 in ATP ($\Delta\delta$ 1.6−6.5 ppm), indicating a lower π-electron density electron density due to adenine substitution.

^{15}N NMR Determination of pK_a Values of Derivatives 1−6. Protonation equilibria of several nucleobases have previously been elucidated by ^{1}H and ^{13}C NMR.[8,20] Yet, ^{15}N NMR is a direct probe for protonation studies of the nucleos(t)ide bases[4c,20b] and allows unambiguous determination of the protonation site. Furthermore, the effects on ^{15}N shifts are much larger than ^{1}H shifts and are therefore less influenced by environmental factors other than base protonation.[2a] In addition, unlike ^{1}H NMR measurements that are performed in D_2O and provide pD values, ^{15}N NMR measurements are performed in H_2O and provide values that are biologically relevant.

On the other hand, a major disadvantage of this spectroscopy is the extremely low sensitivity of ^{15}N at the natural abundance level, which is 3.8×10^{-6} of that of a proton at constant magnetic field.[21] Therefore,^{15}N NMR determination of pK_a values of adenine nucleotides at natural abundance requires concentrated solutions, typically 0.5−1 M. At this concentration range, phenomena that are connected with high concentration such as self-association[22] and high ionic strength should be considered.

We have reported that a 23-fold increase of $(^{15}N)_5$-adenine concentration (from 35 mM to 0.8 M) resulted only in a marginal shift of the nitrogens' ^{15}N chemical shifts (i.e., $\Delta\delta$ of 0.4−1 ppm).[23] The same observation was made with $(^{15}N)_4$-purine riboside; a 75-fold increase of purine riboside concentration (from 13 mM to 0.97 M)

(19) Sierzputowska-Gracz, H.; Wiewiorowski, M.; Kozerski, L.; von Philipsborn, W. *Nucleic Acids Res.* **1984**, *12*, 6247−6258 and references therein.

(20) (a) Liu, M.; Farrant, R. D.; Lindon, J. C.; Barraclough, P. *Spectrosc. Lett.* **1991**, *24*, 1115−1121. (b) Lister, J. H. *The Purines*, Supplement 1; John Wiley: New York, 1996; p 372.

(21) (a) Kanamori, K.; Roberts, J. D. *Acc. Chem. Res.* **1983**, *16*, 35−41. (b) Berger, S.; Braun, S.; Kalinowski, H.-O. *NMR Spectroscopy of the Nonmetallic Elements*; John Wiley: New York, 1996, Chapter 4, pp 229−237.

(22) (a) Scheller, K. H.; Hofstetter, F.; Mitchell, P. R.; Prijs, B.; Sigel, H. *J. Am. Chem. Soc.* **1981**, *103*, 247−260. (b) Scheller, K. H.; Sigel, H. *J. Am. Chem. Soc.* **1983**, *105*, 5891−5900.

(23) Laxer, A.; Major, D. T.; Gottlieb, H.; Fischer, B. *J. Org. Chem.* **2001**, *66*, 5463−5481.

Table 1. ^{15}N NMR Chemical Shifts of ATP Derivatives 1−6

compound	derivative	pH	N1	N3	N7	N9	NH_2
1	ATP	5.24	−164.5	−164.2	−148.9	−211.0	−302.7
2	2-MeS-ATP	5.32	−164.7	−169.6	−151.2	−213.0	−304.0
3	2-$(CH_3)_3CCH_2$S-ATP	5.36	−160.8	−169.1	−150.7	−212.5	−303.7
4	N^6-Me-ATP	5.31	−162.9	−168.6	−150.1	−211.8	−302.4
5	2-Cl-ATP	5.41	−158.0	−166.9	−149.0	−211.0	−297.7
6	8-Br-ATP	5.15	−161.7	−160.6	−141.3	−214.4	−301.3

Table 2. Δδ of Nitrogens Measured at the Beginning and End of Titration of ATP Derivatives

			$\Delta\delta^{obs}$				
compd	derivative	pH range	N1	N3	N7	N9	NH_2
1	ATP	2.05−5.99	−66.4	5.3	4.8	6.9	9.8
2	2-MeS-ATP	2.14−5.94	−51.4	1.5	−2.3	5.9	9.9
3	2-$(CH_3)_3CCH_2$S - ATP	1.90−5.90	−52.2	1.1	−5.0	6.1	9.2
4	N^6-Me-ATP	1.77−6.36	−67.3	8.3	4.3	7.1	11.8
5	2-Cl-ATP	−0.15−5.41	−8.2[a]	2.7	*b*	6.3	7.9
6	8-Br-ATP	1.92−6.09	−62.4	4.8	3.4	7.5	9.0

[a] Titration was stopped at pH −0.15. [b] The chemical shift of N7 was not observed in the acidic range.

Table 3. Fitted Parameters from Titration Curves

compd	derivative	$\Delta\delta(N1)^{extrp}$ [a]	pK_a [b]
1	ATP	−70	4.16
2	2-MeS-ATP	−73	3.22
3	2-$(CH_3)_3CCH_2$S-ATP		3.54
4	N^6-Me-ATP	−73	3.88
5	2-Cl-ATP		−0.2
6	8-Br-ATP	−67	3.83

[a] Full Δδ for N1 were obtained from the fitted asymptotic values of the sigmoid titration curve (e.g., Figure 2). Fitting of the experimental data points to a sigmoid curve was achieved by eq 7. [b] pK_a is the inflection point of the fitted curve (e.g., Figure 2). The inflection point was determined by calculating the second derivative of the fitted curve. The estimated error for pH meter reading is ±0.02, except for reading below pH 0 (i.e., last measurement at pH −0.15 for compound **5**).

had a negligible effect on the corresponding ^{15}N NMR spectra (i.e., Δδ of 0.7−0.8 ppm).[24] These minor changes of chemical shifts indicate that base stacking and H-bonding are limited at 0.8−1 M nucleoside concentrations and/or do not influence ^{15}N NMR chemical shifts. On the other hand, protonation of N1 leads to a huge upfield shift of ca. 70 ppm. In any case, the overwhelmingly large Δδ of N1 masks environmental factors that are about 2 orders of magnitude smaller.

In addition, Sigel et al. have shown that self-association in nucleotides decreases considerably by going from adenosine to ATP.[4,22] Therefore, we intended to deduce pK_a values of adenine nucleotides with ^{15}N NMR in a facile way in H_2O at natural abundance, expecting only a marginal error under these experimental conditions.

Solutions of trisodium salts of the nucleotide derivatives **1**−**6**, at pH 6, were titrated with dilute hydrochloric acid at 25 °C, and their ^{15}N NMR spectra were recorded at 60.8 MHz. Changes of ^{15}N NMR spectra as a function of the pH were monitored, and a gradual upfield shift of N1 was noted (Figure 1).

The increased acidity of the solution caused changes in all nitrogens' chemical shifts (Table 2). The most pronounced change was an upfield shift of N1 of ca. 70 ppm, indicating an increase of its sp^3 character due to protonation (Table 3). A downfield shift of 9−10 ppm of the exocyclic amine is attributed to its increased sp^2 character. This is readily seen in the mesomeric structures stabilizing the formed cationic nucleotide species. This effect is most pronounced (Δδ 12 ppm) for N^6-Me-ATP. The positive inductive effect of the methyl group renders the lone electron pair of N^6-amine more available to mesomeric stabilization of the protonated adenine ring. The positive inductive effect of the methyl group is also reflected in a significant N3 upfield shift with Δδ of 8.3 ppm.

Plotting the chemical shift of N1 vs pH provides a sigmoid curve (e.g., Figure 2, for derivative **6**). The pK_a value is obtained from the inflection point, which is determined by the second derivative of the fitted sigmoid function (Figure 3). In this way, pK_a values were obtained for derivatives **1**−**6** (Table 3). The observed pK_a value for ATP was 4.16. This is in a good agreement with reported pK_a values obtained by other methods: 4.15,[25] 4.10,[26] and 4.03.[4a]

pH titration of most of the samples resulted in a drastic upfield shift in the N1 chemical shift, whereas the signals of other adenine nitrogens (N3, N7, N9, N^6) are slightly moved downfield (Table 2), reflecting the electron poor nature of the protonated ring system. For derivatives **2** and **3** we observed an upfield shift also for N7, although less than that for N1 (Table 2). This finding indicates the existence of an N7 singly protonated species in addition to the N1−H^+ form. Strong electron-donating groups at C8 are known to induce protonation of the adenine ring at N7 in addition to N1.[12a] Here, we find that strong electron-donating groups at C2 have practically the same effect.

The ^{15}N NMR method is suitable for the determination of acidity constants of nucleoside-triphosphate derivatives but not of the corresponding monophosphate analogues, because of their low solubility in acidic solutions. AMP, for instance, precipitates out of solution at pH 4. Clearly, this method is not applicable to nucleosides as a result of their extremely low solubility in aqueous solutions.

Because of the low sensitivity of natural abundance ^{15}N NMR, one must use 0.5−1 M solutions of nucleotides in water for the determination of pK_a values. This requirement makes this method impractical for cases where such concentrations are not readily available. Therefore, we developed a simple theoretical procedure for the prediction of pK_a values of modified adenine bases. Once this method reproduces the substituent-dependent variations in experimentally determined pK_a values of nucleotides, we can apply this method to the prediction

(24) Laxer, A.; Fischer, B. Unpublished results.

(25) Watanabe, S.; Evenson, L.; Gulz, I. *J. Biol. Chem.* **1963**, *238*, 324−327.

(26) Tribolet, R.; Sigel, H. *Eur. J. Biochem.* **1988**, *170*, 617−626.

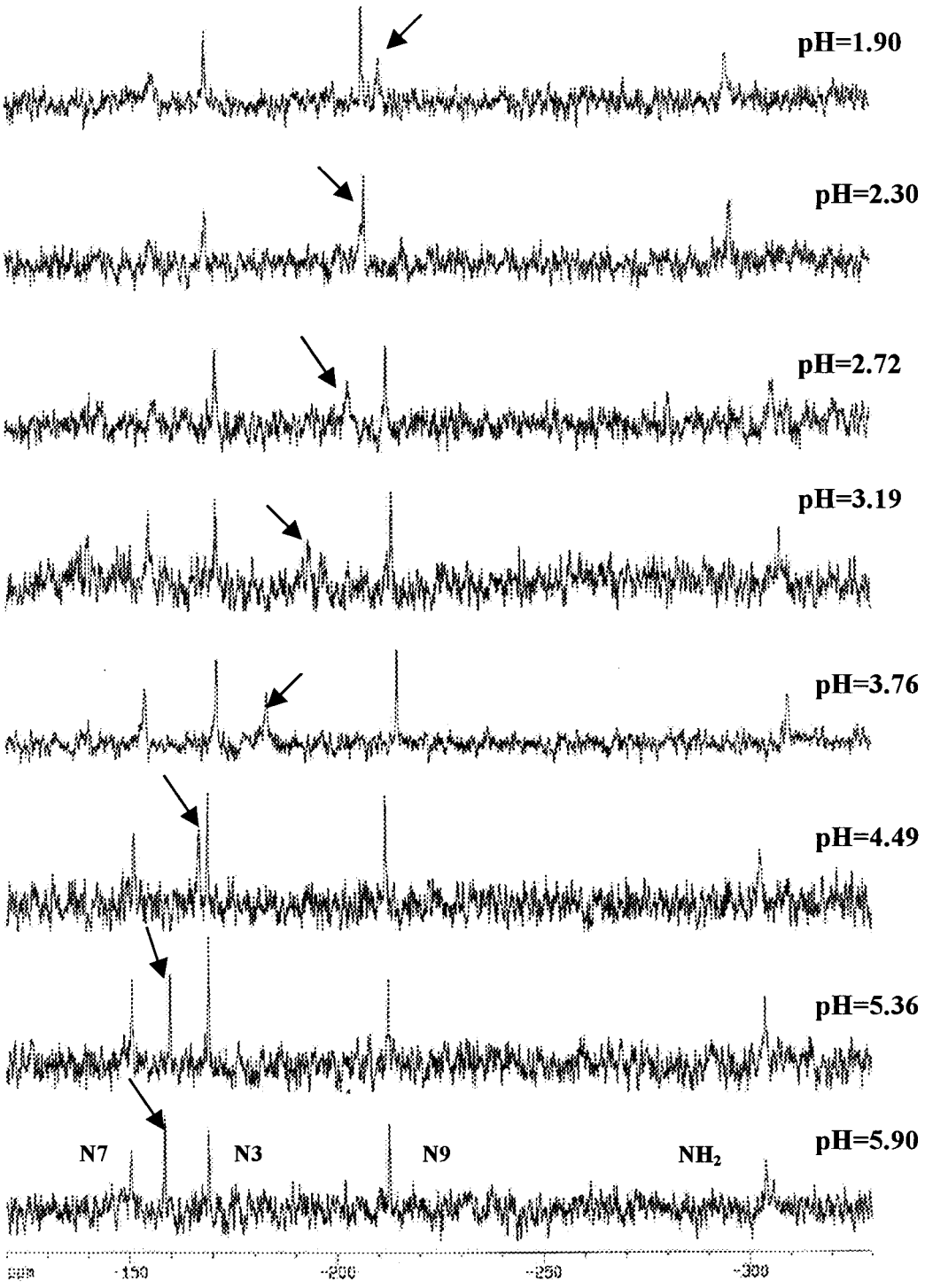

Figure 1. Changes of ^{15}N NMR spectra of 2-(2,2-dimethylpropyl)thio-ATP, **3**, as a function of pH (N1 is marked by an arrow), recorded at 60.8 MHz, 0.91 M, 25 °C.

of pK_a values of novel chemically modified nucleobase derivatives. Furthermore, this method should enable the prediction of the preferential protonation site(s) (e.g., N1/N7/N3) and may help rationalize adenine substituent effects on pK_a.

Theoretical Calculation of pK_a Values of Substituted Adenine Bases. Several theoretical studies on the determination of pK_a of various organic compounds have been reported.[27] These studies include the calculation of the pK_a of individual molecules such as amines,[27g] nitriles,[27h] hydroxybenzoic acids,[27i] carboxylic acids,[27j] uracil derivatives,[27p] and model amino acid residues.[27d] Other models for the calculation of pK_a values were developed for transition states and intermediates, as in the enzymatic methylation of cytosine,[27k] or pK_a values of acetic acid during α-proton abstraction.[27l]

The free energy of protonation in solution is related to the pK_a by the following expression:

$$\mathrm{p}K_a = \frac{1}{2.303RT}\Delta G_{aq}^{prot} \qquad (1)$$

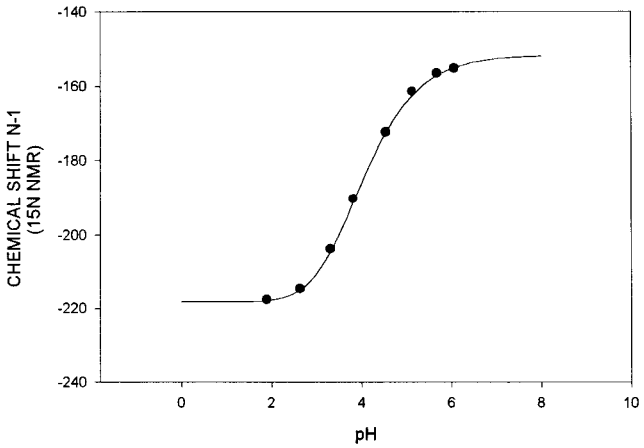

Figure 2. Changes of N1 ^{15}N chemical shift vs pH in 8-Br-ATP, **6**. A 0.9 M solution of 8-Br-ATP at pH 6.09 was titrated with dilute HCl at 25 °C, and changes of ^{15}N NMR spectra (at 60.8 MHz) were monitored as a function of pH.

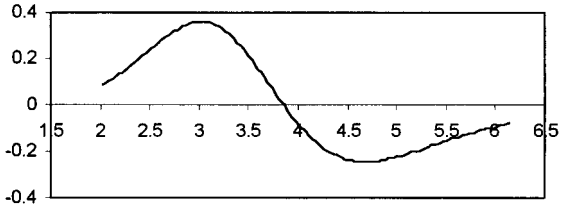

Figure 3. Determination of pK_a for 8-Br-ATP based on the second derivative of the fitted sigmoid curve (shown in Figure 2).

The free energy of protonation in aqueous solution, ΔG_{aq}^{prot}, may be calculated using a thermodynamic cycle:

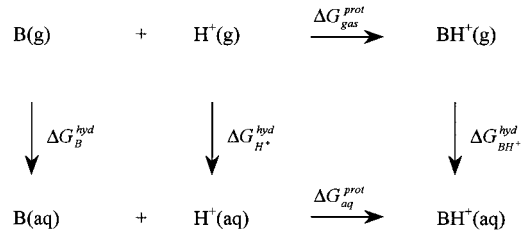

$$\Delta G_{aq}^{prot} = \Delta G_{gas}^{prot} + \Delta G_{BH^+}^{hyd} - \Delta G_{B}^{hyd} - \Delta G_{H^+}^{hyd} = \Delta G_{gas}^{prot} + \Delta\Delta G^{hyd} \quad (2)$$

The gas-phase protonation free energy is usually obtained from quantum mechanical calculations, while the free energy of hydration may be calculated by discrete solvent models or by continuum models. Most theoretical approaches differ concerning solvent treatment. For this treatment several solvation models exist, each having its strengths and weaknesses. Some of the discrete solvation methods used in pK_a calculations include free energy perturbation simulations in explicit water[27b,c,e] and the Langevin dipole model.[27a] On the other hand, the commonly used continuum models are based on the Born model,[27f] the Poisson−Boltzmann (PB) equation,[27d,p] and various implementations of the polarizable continuum model (PCM).[27g−l] The advantage of continuum models over discrete methods is that the solvent reaction field may be incorporated into the quantum mechanical Hamiltonian, and thus an accurate description of the solvated solute may be achieved.

The computation of accurate, absolute pK_a values is a demanding task as a result of errors both in the calculated gas-phase free energy of protonation and free energy of solvation.[28] An error of 1.36 kcal/mol in the calculated free energy of protonation leads to a pK_a shift of about one pK_a unit.

However, Jang and Goddard III et al. recently reported first principles calculation of pK_a values for 5-substituted uracils.[27p] This work presented an important step toward the prediction of accurate first principles pK_a values. Nonetheless, the free energy of solvation of the proton, for which several experimental values exist, was explicitly fitted to reproduce the experimental pK_a values for the 5-substituted uracil series. Moreover, the dielectric constant used to represent the quantum mechanical region within the Poisson−Boltzmann continuum model was fitted to reproduce the experimental pK_a values. Thus, it is questionable whether this model would correctly predict pK_a values for other heterocycles unless new parameters are developed.

An alternative approach involves the calculation of semiempirical pK_a values.[27k,l] This can be performed by calculating the free energy of protonation in aqueous solution (eq 2) and pK_a values (eq 1) for a range of compounds with known experimental pK_a values. The calculated pK_a values, which contain systematic errors inherent to the computational methods, may be fitted to the experimental ones by a linear regression analysis leading to the following correlation equation:

$$pK_a^{exp} = a \cdot pK_a^{calc} + b \quad (3)$$

Accurate, "experimental-like" pK_a values of new compounds may then be predicted using the linear equation obtained.

The goal of this theoretical study is to determine and rationalize the accurate, experimental-like pK_a values of nitrogen heterocycles of biological importance. In particular, the pK_a values of derivatives of adenine (Scheme 4) were calculated, and the substituent-dependent variations in these pK_a values were compared with the experimental results for the corresponding ATP derivatives (Scheme 1). Moreover, the influence of ED and EW substituents on the pK_a of adenine derivatives **12**−**22** was investigated, as well as the localization of the protonation site(s) on the molecule and the identification of the major protonated species. This approach is complementary to the experimental data presented above for ATP deriva-

(27) (a) Warshel, A. *Biochemistry* **1981**, *20*, 3167−3177. (b) Jorgensen, W. L.; Briggs, J. M.; Gao, J. *J. Am. Chem. Soc.* **1987**, *109*, 6857−6858. (c) Jorgensen, W. L.; Briggs, J. M. *J. Am. Chem. Soc.* **1989**, *111*, 4190−4197. (d) Lim, C.; Bashford, D.; Karplus, M. *J. Phys. Chem.* **1991**, *95*, 5610−5620. (e) Gao, J.; Pavelites, J. J. *J. Am. Chem. Soc.* **1992**, *114*, 1912−1914. (f) Yang, B.; Wright, J.; Eldefrawi, M. E.; Sovitj, P.; MacKerell, A. D., Jr. *J. Am. Chem. Soc.* **1994**, *116*, 8722−8732. (g) Kallies, B.; Mitzner, R. *J. Phys. Chem. B* **1997**, *101*, 2959−2967. (h) Colominas, C.; Orozco, M.; Luque, F. J.; Borrel, J. I.; Teixidó, J. *J. Org. Chem.* **1998**, *63*, 4947−4953. (i) Shapley, W. A.; Bacskay, G. B.; Warr, G. G. *J. Phys. Chem. B* **1998**, *102*, 1938−1944. (j) Schüürmann, G.; Cossi, M.; Barone, V.; Tomasi, J. *J. Phys. Chem. A* **1998**, *102*, 6706−6712. (k) Peräkylä, M. *J. Am. Chem. Soc.* **1998**, *120*, 12895−12902. (l) Peräkylä, M. *Phys. Chem. Chem. Phys.* **1999**, *1*, 5643−5647. (m) Gargallo, R.; Sotriffer, C. A.; Liedl, K. R.; Rode, B. M. *J. Comput.-Aided Mol. Des.* **1999**, *13*, 611−623. (n) Güven, A.; Yekeler, H.; Özkan, R. *J. Mol. Struct. (THEOCHEM)* **2000**, *499*, 13−19. (o) Alkorta I.; Gonzales, E.; Jagerovic, N.; Elguero, J.; Flammang, R. *J. Phys. Org. Chem.* **2000**, *13*, 372−381. (p) Jang, Y. H.; Sowers, L. C.; Çağin. T.; Goddard, W. A., III. *J. Phys. Chem. A* **2001**, *105*, 274−280.

(28) Cramer, C. J.; Truhlar, D. G. *Chem. Rev.* **1999**, *99*, 2161−2200.

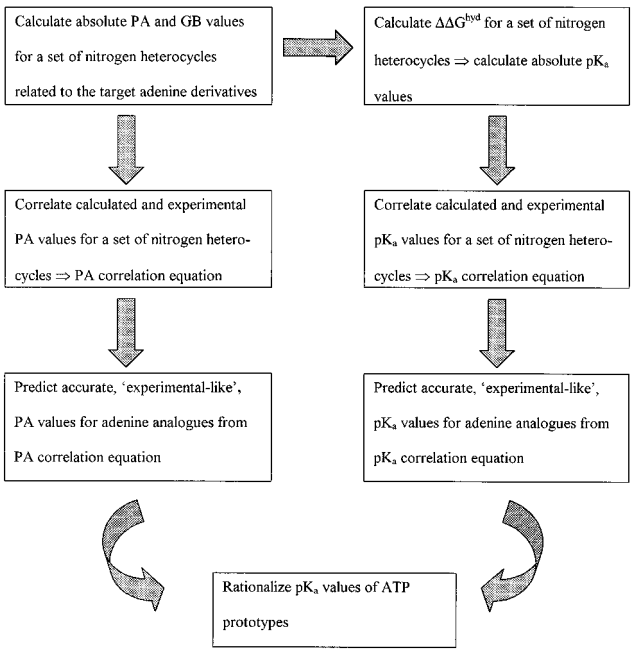

Figure 4. Schematic representation of the computational strategy adopted to explain the substituent-dependent variation in pK_a of the investigated ATP prototypes.

Scheme 4

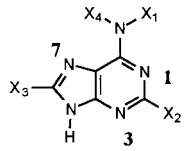

12 X_1=X_2=X_3=X_4 =H
13 X_1=X_3=X_4 =H, X_2=SCH_3
14 X_1=X_3=X_4 =H, X_2=$SCH_2C(CH_3)_3$
15 X_1=CH_3, X_2=X_3=X_4 =H
16 X_1=X_3=X_4 =H, X_2=Cl
17 X_1=X_2=X_4 =H, X_3=Br
18 X_1=X_3=X_4 =H, X_2=$NHCH_3$
19 X_1=X_2=X_4 =H, X_3=NH_2
20 X_1=X_4 =CH_3, X_2=X_3=H
21 X_1=X_2=X_4 =H, X_3=Cl
22 X_1=X_2=X_4 =H, X_3=SCH_3

tives **1**−**6**. This approach can also provide predicted pK_a values for adenine analogues where it is impossible to obtain these values by experiment and provide pK_a values of novel derivatives that have not been synthesized.

Computational Strategy. The current approach, combining DFT and PCM[29] calculations for the prediction and interpretation of adenine pK_a values, involved the following four steps (Figure 4): (A) Calculating the gas-phase proton affinity (PA) for a set of 16 heterocycles (**12**, **23**−**28**, **34**, **36**−**43**, Table 4) for which experimental PAs are available. These heterocycles are structurally related to the target adenine derivatives (**12**−**22**). The computed PAs were correlated with experimental values. (B) Predicting accurate, experimental-like PAs for the target adenine derivatives (**12**−**22**) on the basis of results obtained in A. (C) Calculating $\Delta\Delta G^{hyd}$and pK_a values for a set of 23 heterocycles (**12**, **23**−**44**, Table 4) related to the target adenine derivatives (**12**−**22**). These computed pK_a values were correlated with experimental values (eq 3). In this approach, the atomic radii used to build up the molecular cavity within PCM were fitted to reproduce the experimental pK_a values. (D) Predicting accurate, experimental-like pK_a values of the adenine derivatives (**12**−**22**), using the correlation equation obtained in C.

(29) Miertus, S.; Scrocco, E.; Tomasi, J. *Chem. Phys.* **1981**, *55*, 117−129.

Table 4. Computed and Experimental Gas-Phase Proton Affinities (PA, kcal/mol) and pK_a Values of Various Heterocycles Used To Create the Linear PA and pK_a Correlation Equations[a]

compd	derivative	PA^{calc} [b]	PA^{exp} [c]	pK_a^{calc} [d]	pK_a^{exp} [e]
12	adenine	224.3	225.3	3.95	4.12
23	purine	220.6	219.9	2.56	2.3
24	cytosine	226.6	227.0	4.47	4.5
25	uracil	206.4	207.1	9.39	9.5
26	thymine	208.0	209.0	9.72	9.9
27	guanine	227.2	227.4	3.31	3.3
28	imidazole (Im)	224.2	225.3	6.37	6.95
29	4-Cl-1-Me-Im	nd[f]	nd[f]	2.63	3.1
30	4-Br-Im	nd[f]	nd[f]	3.22	3.6
31	2-Br-Im	nd[f]	nd[f]	3.31	3.85
32	thiazole	nd[f]	nd[f]	2.54	3.44
33	2- NH_2-thiazole	nd[f]	nd[f]	5.48	5.36
34	pyrimidine	212.8	211.7	1.77	1.3
35	2-NH_2-pyrimidine	nd[f]	nd[f]	3.89	3.45
36	pyrazine	210.3	209.6	0.88	0.65
37	pyridine	222.1	222.0	5.24	5.25
38	2-NH_2-pyridine	226.6	226.4	7.10	6.82
39	3-NH_2-pyridine	228.2	228.1	6.40	6
40	4-NH_2-pyridine	234.0	234.2	9.10	9.11
41	2-Me-pyridine	226.3	226.8	6.04	5.97
42	3-Me-pyridine	225.4	225.5	5.72	5.68
43	4-Me-pyridine	226.4	226.4	5.95	6.02
44	pyrrole	nd[f]	nd[f]	17.65	17.5
corr coeff[g]		0.994		0.993	
slope[g]		0.89		0.81	
intercept[g]		24.16		−0.19	
rms error[h]		0.625		0.29	

[a] Figures 5 and 6. [b] PA computed according to eqs 4−6. The electronic energy was calculated at the B3LYP/aug-cc-pVTZ(-f)//B3LYP/6-31G(d,p) level. The thermal corrections were computed at the B3LYP/6-31G(d,p) level. The computed PAs were obtained from a linear regression equation of the form $PA^{exp} = a \cdot PA^{calc} + b$. [c] Experimental data was taken from ref 33. [d] pK_a computed according to eqs 1−3 at the B3LYP/aug-cc-pVTZ(-f)-PCM-pK_a level. The computed pK_a values were obtained from a linear regression equation of the form $pK_a^{exp} = a \cdot pK_a^{calc} + b$. [e] Experimental data was taken from ref 36. [f] Not determined. [g] Data for linear regression equations. [h] Root-mean-square error (kcal/mol and pK_a units) in calculated values.

These results were, in turn, utilized to explain the trend in the substitution-dependent experimental pK_a values for the corresponding ATP derivatives (**1**−**6**). The results of steps A and C are presented in Table 4 and Figures 5 and 6, while the results of steps B and D are presented in Table 5.

(A) Calculation of Gas-Phase Proton Affinity for a Calibration Set of Heterocycles. A prerequisite to rationalize the basicity of nucleic acid bases in a given medium is to understand their inherent basicity in the gas phase. The basicity of a given base, B, in the gas phase may be described by its PA. The PA is defined as the negative of the enthalpy of protonation of B:

$$B(g) + H^+(g) \xrightarrow{\Delta H^{prot}_{gas}} BH^+(g)$$

$$PA = -\Delta H^{prot}_{gas}(T) \quad (4)$$

$$\Delta H^{prot}_{gas}(T) = \Delta E^{prot}_{elec} + \Delta E^{prot}_{zpe} + \Delta E^{prot}_{vib}(T) + \frac{5}{2} RT \quad (5)$$

The gas-phase protonation enthalpy, $\Delta H^{prot}_{gas}(T)$, is defined as the difference in electronic energy, ΔE^{prot}_{elec}, zero-

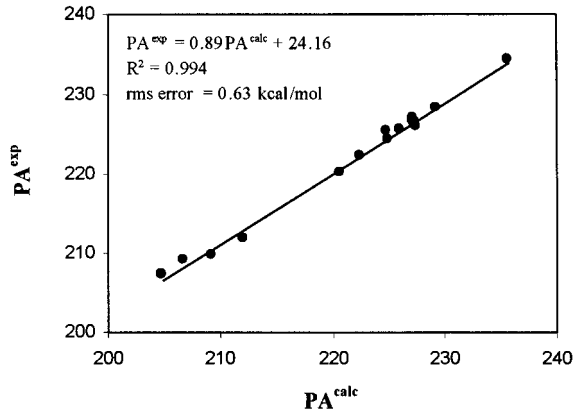

Figure 5. Correlation between the calculated and the corresponding experimental gas-phase proton affinities (PA) for heterocycles **12**, **23**−**28**, **34**, and **36**−**43** (Table 4). PA was computed according to eqs 4−6.

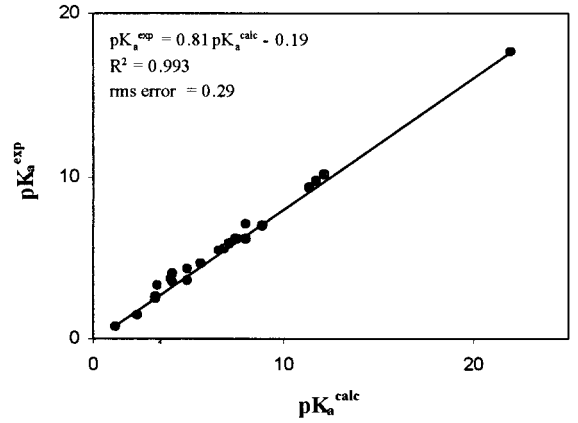

Figure 6. Correlation between the calculated and the corresponding experimental pK_a values for heterocycles **12** and **23**−**44** (Table 4). pK_a was computed according to eqs 1−3. The PCM atomic radii were fitted to reproduce experimental pK_a values (Table 6).

point energy, ΔE_{zpe}^{prot}, and vibrational energy, $\Delta E_{vib}^{prot}(T)$, between the protonated and unprotonated species. The $^5/_2RT$ term includes the translation energy of the proton and the Δ(PV) term. Analogous to the PA, the gas-phase basicity (GB) is defined as $-\Delta G_{gas}^{prot}$.

In a recent comprehensive post-Hartree−Fock (HF) study, accurate PA values for nucleic acid bases were calculated.[30] However, post-HF methods are still expensive from a computational point of view. It has previously been shown that the B3LYP functional[31] yields reasonable PAs for nucleic acid bases.[32] Thus, we decided to use the far more economical B3LYP DFT method.

The ability of the B3LYP functional to reproduce the experimental PA values was examined for a set of 16 heterocycles (**12**, **23**−**28**, **34**, **36**−**43**) for which experimental PA values are available (Table 4).[33] These heterocycles are structurally related to the target adenine analogues. The B3LYP functional was chosen together with the cc-pVTZ(-f) and aug-cc-pVTZ(-f) basis sets.[34] The latter basis set includes diffuse functions on all atoms. The selected set of heterocycles span a range of PAs from 207.1 to 234.2 kcal/mol. For the five natural nucleic acid bases (**12**, **24**−**27**) only the most stable gas-phase tautomer was considered, as inclusion of rare tautomers has minimal influence on the calculated PA.[30] The results are presented in Table 4.

Table 5. Predicted PA, GB, $\Delta\Delta G^{hyd}$ (all kcal/mol), and pK_a Values for N1 Protonation of Various Adenine Derivatives

compd	derivative	PA[a]	GB[b]	$\Delta\Delta G^{hyd}$ [c]	pK_a[d]
12	adenine (Ad)	224.3	218.5	211.45	3.95
13	2-MeS-Ad	228.9	221.8	216.02	3.25
14	2-$(CH_3)_3CCH_2$S-Ad	231.3	224.7	nd[e]	nd[e]
15	N^6-Me-Ad	228.8	222.6	215.97	3.71
16	2-Cl-Ad	221.4	212.3	212.83	−0.50
17	8-Br-Ad	223.3	217.3	210.36	3.93
18	2-MeNH-Ad	229.2	224.0	214.27	5.55
19	8-NH_2-Ad	231.2	227.1	216.6	6.06
20	N^6-diMe-Ad	231.1	224.3	217.74	3.71
21	8-Cl-Ad	223.8	216.2	209.33	3.89
22	8-MeS-Ad	227.7	222.2	215.10	4.02

[a] PA computed according to eqs 4−6. The electronic energy was calculated at the B3LYP/aug-cc-pVTZ(-f)//B3LYP/6-31G(d,p) level. The thermal corrections were computed at the B3LYP/6-31G(d,p) level. The computed PAs were obtained from a linear regression equation of the form $PA^{exp} = a \cdot PA^{calc} + b$, with the coefficients found in Table 4. [b] The gas-phase basicity (GB) was defined as $-\Delta G_{gas}^{prot}$. [c] Free energy of solvation was calculated using PCM-pK_a-B3LYP/6-31G(d,p). [d] pK_a computed according to eqs 1−3 at the B3LYP/aug-cc-pVTZ(-f)-PCM-pK_a level. The computed pK_a values were obtained from a linear regression equation of the form $pK_a^{exp} = a \cdot pK_a^{calc} + b$, with the coefficients found in Table 4. [e] Not determined.

The absolute PAs obtained with the B3LYP/aug-cc-pVTZ(-f) functional agree more closely with the experimental values than B3LYP/cc-pVTZ(-f). The root-mean-square errors were 1.24 and 2.16 kcal/mol, respectively. However, these errors are partly due to systematic errors in the calculated PA values. The results may be improved if relative PAs are calculated instead of absolute values. Thus, a linear regression analysis was performed (Figure 5) where the experimental and calculated PAs were related by the following equation:

$$PA^{exp} = a \cdot PA^{calc} + b \qquad (6)$$

The R^2 values obtained were 0.994 and 0.986 with and without diffuse functions, respectively. The root-mean-square errors were 0.63 and 0.88 kcal/mol, respectively. The values obtained are well within the estimated experimental error of 2 kcal/mol.[33]

(B) Calculation of Gas-Phase Proton Affinity for Substituted Adenine Derivatives. From the linear regression analysis equation obtained (Figure 5), it is possible to predict the expected experimental PAs of the investigated adenine derivatives (**12**−**22**, Table 5).

For all cases, only the N^6-amino adenine tautomer was considered since it is far more stable than the imino tautomers.[14d] Likewise, only the N9-H adenine tautomer

(30) Podolyan, Y.; Gorb, L.; Leszczynski, J. *J. Phys. Chem. A* **2000**, *104*, 7346−7352.
(31) (a) Lee, C.; Yang, W.; Parr, R. G. *Phys. Rev. B: Condens. Matter* **1988**, *37*, 785−789. (b) Miehlich, B.; Savin, A.; Stoll, H.; Preuss, H. *Chem. Phys. Lett.* **1989**, *157*, 200−206. (c) Becke, A. D. *J. Chem. Phys.* **1993**, *98*, 5648−5652.
(32) (a) Russo, N.; Toscano, M.; Grand, A.; Jolibois, F. *J. Comput. Chem.* **1998**, *19*, 989−1000. (b) Wolken, J. K.; Tureèek, F. *J. Am. Soc. Mass. Spectrom.* **2000**, *11*, 1065−1071.
(33) Hunter, E. P. L.; Lias, S. G. *J. Phys. Chem. Ref. Data* **1998**, *27*, 413−656.
(34) (a) Dunning, T. H. *J. Chem. Phys.* **1989**, *90*, 1007−1023. (b) Kendall, R. A.; Dunning, T. H.; Harrison, R. J. *J. Chem. Phys.* **1992**, *96*, 6796−6806. (c) Woon, D. E.; Dunning, T. H. *J. Phys. Chem.* **1993**, *98*, 1358−1371.

was considered since this is the major tautomer in equilibrium in solution.[23] In addition, only pK_a values calculated for the N9-H tautomer are relevant when analyzing effects on acidity constants of adenine nucleotides, where the N9 position bears a phosphorylated ribose.

N1 was found to be the favored site of protonation in the gas phase for all the derivatives (results not shown).[14d] Table 5 presents the results obtained using B3LYP/aug-cc-pVTZ(-f). The PA of adenine, which is included in the calibration set, is predicted to be 224.3 kcal/mol, close to the experimental value with an error of 1 kcal/mol. The PA of 2-MeS-adenine is increased by 4.6 kcal/mol relative to adenine, clearly revealing the strong ED character of the thioether group. In 2-$(CH_3)_3CCH_2$S-adenine, this effect is even more pronounced as is expected by the greater ED effect of the 2,2-dimethylpropyl group. A strong ED effect is also observed for 2-MeNH-adenine, where the PA for N1 protonation is almost 5 kcal/mol greater than that of the parent compound. On the other hand, the 2-Cl-adenine derivative is less basic than adenine by more than 3 kcal/mol as a result of the EW effect of the chlorine atom. The ED effect of the methylthio group is reduced when the substitution is at the C8-position rather than at C2. In this case, the PA is increased by only 3.4 kcal/mol compared to adenine. If adenine is substituted at the C8 position with an NH_2 group the PA is increased by 6.9 kcal/mol. An EW effect is observed in 8-Cl-adenine, albeit smaller than for 2-Cl-adenine because of the more remote position of the chlorine atom. The N^6-Me-adenine derivative shows increased basicity of N1 as a result of an ED effect. The PA is further increased if an additional methyl is added to N^6.

(C) Creating the Linear pK_a Equation. The free energy of protonation in aqueous solution was calculated according to eq 2. The gas-phase part of the protonation free energy was calculated using the B3LYP functional with the aug-cc-pVTZ(-f) basis set. The difference in free energy of hydration was calculated using the polarizable continuum model. The free energy of solvation in continuum solvation models may be written

$$\Delta G^{\mathrm{solv}} = \Delta G^{\mathrm{es}} + \Delta G^{\mathrm{cav}} + \Delta G^{\mathrm{dis-rep}} \qquad (7)$$

where the superscripts stand for electrostatic, cavitation, and dispersion-repulsion. The electrostatic contribution to the solvation free energy is represented quantum mechanically and accounts for the mutual polarization of the solute and solvent. The polarization of the solvent due to the solute is reproduced by a set of point charges distributed on the molecular cavity (i.e., the reaction field). This reaction field induces a polarization of the solute charge distribution, and the solute in turn polarizes the solvent. This process is continued until self-consistency is achieved. The solute−solvent interaction is dependent upon the shape and size of the molecular cavity. A cavity that is too small will overestimate the solute−solvent interaction, while too-large a cavity will underestimate this interaction. Thus, a crucial parameter in continuum models is the definition of the molecular boundary. In PCM, the solute is embedded in a cavity of molecular shape surrounded by a continuous dielectric medium. The cavity is formed by a set of interlocking spheres centered on the solute nuclei, and the radii of each sphere is usually taken as the van der Waals (vdW) radii. In the calculation of the electrostatic part of the solvation energy, each atomic radius is multiplied by a scaling factor so that it mimics the first hydration shell.[35] An advantage of using the scaling factor is that it is used only in the calculation of the electrostatic part of the solvation energy. Thus, it may be changed in order to fine-tune the electrostatic interaction between solvent and solute.

Table 6. Scaling Factors for the Pauling vdW Radii Set Fitted To Reproduce Experimental pK_a Values of Nitrogen Heterocycles (12, 23−46)

atom	vdW radii (Å)	scaling factor
H	1.2	1.2
H (polar)	1.2	1.0
C	1.5	1.35
N	1.5	1.0
O	1.4	1.0
S	1.85	1.0
Cl	1.80	1.2
Br	1.95	1.2

Usually the atomic radii or the scaling factors are fitted to reproduce experimental solvation energies. For neutral species, this leads to very accurate results.[35] However, for ions, the experimental solvation energies are not very accurate because of the large absolute values. Experimental pK_a values, on the other hand, are usually obtained with high accuracy. Thus, calculated pK_a may be greatly improved by fitting the PCM atomic radii to reproduce experimental pK_a values (denoted PCM-pK_a).

The scaling factors for the relevant atoms in derivatives **12**−**22** were optimized to reproduce experimental pK_a values, and the results are shown in Table 6. A description of the fitting process of the atomic radii appears in Methods.

A set of 23 heterocycles with known pK_a values[36] (Table 4) were included in the calibration set to assemble a linear relationship between the experimental and the calculated pK_a values (Figure 6). The selection of the calibration set was based on the following criteria: (A) Heterocycles that are structurally related to the target molecules of this study (i.e., adenine derivatives), namely, pyridines, pyrimidines, imidazoles, and purines. Two thiazoles were also included to allow the parametrization for sulfur. (B) Heterocycles that span a wide range of pK_a (i.e., 0.65−17.5). (C) Even distribution of pK_a values within the range of 0.65−17.5.

A study by Peräkylä showed that different functional groups have inherent systematic errors in the calculated energies.[27k,l] These systematic errors may be due to errors in the calculated hydration energies. Marten et al. suggested that systematic errors in solvation energies are due to nonelectrostatic hydrogen bonding properties and are related to the acid/base properties of hydrogen bond donors and acceptors.[37] Thus, the best results may be

(35) Bachs, M.; Luque, F. J.; Orozco, M. *J. Comput. Chem.* **1994**, *15*, 446−454.

(36) (a) *CRC Handbook of Chemistry and Physics*, 8th ed.; Lide, D. R., Ed.; CRC Press: Boca Raton, FL, 1999−2000. (b) Grimmett, M. R. In *Comprehensive Heterocyclic Chemistry. The Structure, Reactions, Synthesis and Uses of Heterocyclic Compounds*; Katritzky, A. R., Rees, C. W., Eds.; Pergamon Press Ltd.: Oxford, 1984; Vol. 5, p 384.

(37) Marten, B.; Kim, K.; Cortis, C.; Friesner, R. A.; Murphy, R. B.; Ringnalda, M. N.; Sitkoff, D.; Honig, B. *J. Phys. Chem.* **1996**, *100*, 11775−11788.

obtained by choosing a set of compounds that have related structures, where the systematic errors are similar.

A range of pK_a values, as wide as possible, was sought to allow wider application of the linear pK_a equation. Hence, the protonation of both neutral species (e.g., adenine) and anions (e.g., uracil) was investigated. In addition, molecules with several tautomeric structures (e.g., purine, adenine, guanine, cytosine, uracil, and thymine) were included, to investigate the robustness of the equation. In these cases, the most stable tautomer in solution was considered. For purine and adenine the N9-H tautomer was used.[38a] In the case of guanine and cytosine, the amino-oxo tautomer was considered,[38a,b] and for uracil and thymine the di-oxo tautomer was considered.[38b] However, no molecules with conformational flexibility (i.e., nucleosides, nucleotides) were included, as this would greatly complicate the creation of the pK_a equation.

Table 4 and Figure 6 present the calculated pK_a values obtained with the PCM-pK_a parametrization. Using PCM-pK_a, an R^2 value of 0.993 was found and the rms error was 0.29 pK_a units, which corresponds to 0.40 kcal/mol. The largest and most systematic errors for the calibration set are found for the imidazole series, where the pK_a is overestimated by 0.38−0.59 pK_a units. This indicates that the atomic radii scaling factors may be improved for imidazoles.

The importance of choosing appropriate atomic radii scaling factors is clearly seen when comparing the results obtained with the PCM-pK_a parametrization with results obtained using two other models: PCM-UAHF[39] at the HF/6-31G(d,p) level, and PCM with B3LYP/6-31G(d,p) and the Pauling atomic radii set with standard scaling factors (1.2 for all atoms except for polar hydrogens where a scaling factor of 1.0 is used). PCM-UAHF provided excellent pK_a values for carboxylic acids in a study by Schüürmann et al. with correlation coefficients of 0.97 and standard error of 0.24 pK_a units.[27j] Therefore, the PCM-UAHF model was tested in this study to evaluate its performance for heterocycles. However, PCM-UAHF leads to a correlation coefficient of only 0.879 and a large rms error of 1.22 pK_a units. Using the Pauling radii set with standard scaling factors, a correlation coefficient of 0.922 and rms error of 1.04 pK_a units were found. It is thus clear that the fitting of the scaling factors, used in the creation of the molecular cavity to reproduce experimental pK_a values, greatly improves the results. Reducing the scaling factor for the hydrogen-bonding atoms (N, O, H, S) to about 1.0 compared to the standard scaling factor of 1.2 led to results closest to experimental pK_a values (Tables 5 and 6). Reduced scaling factors correspond to a stronger interaction between solute and solvent. This may be necessary to compensate for non-electrostatic effects in solvation, such as charge transfer, which continuum models cannot take into account. Moreover, the PCM-pK_a parametrization is simple, and uses a single scaling factor for each atom type.

(D) Predicted pK_a Values for Adenine Derivatives. The pK_a values of 11 adenine derivatives (Scheme 4, **12**−**22**) were predicted with the linear pK_a equation (eqs 1−3) using the PCM-pK_a scaling factors in the solvation calculations (Table 5).

As mentioned above, in all of the neutral adenine derivatives, the N9-H amino tautomer is the major and relevant one for comparison of pK_a values with adenine nucleos(t)ides. Additionally, the ^{15}N NMR spectra show that protonation occurs at the N1 position, except for 2-MeS- and 2-$(CH_3)_3CCH_2$S-ATP, where N7 protonation also occurs. It has also been shown for 8-NH_2-adenosine that the most basic site on the adenine ring is N7.[12a] Thus, with the exception of 2-MeS-adenine and 8-NH_2-adenine, only the N9-H amino tautomer and its N1 protonated conjugated acid will be discussed.

The calculated pK_a of adenine, which is included in the calibration set, is very close to the experimental value with an error of only 0.17 pK_a units. Substitution at the C2 position of the adenine ring with a chlorine atom leads to a dramatic decrease in pK_a, with a predicted value of −0.5. The pK_a of 2-MeNH-adenine is increased relative to adenine by 1.6 pK_a units. Surprisingly, the pK_a of 2-MeS-adenine is lowered relative to adenine. Replacing the N^6-hydrogens with one or two methyl groups decreases the basicity of N1. The substitutions at the C8-position with chlorine and bromine led to calculated pK_a values similar to those of adenine, with values of 3.89 and 3.93, respectively. The 8-MeS-adenine is predicted to have a pK_a very similar to that of adenine, although its PA is greater than that of adenine. On the other hand, the N7 nitrogen in 8-NH_2-adenine is found to be substantially more basic than N1 in adenine. N7 protonation in 8-NH_2-adenine is found to be slightly more favorable than N1 protonation; the difference between N1 and N7 protonation being less than 0.5 kcal/mol. That is, for 8-NH_2-adenine a mixed population of monoprotonated species is expected.

Comparison of the calculated pK_a values for the above-mentioned adenine derivatives with corresponding experimental values is not feasible because of the low solubility of these compounds in water. However, it may be instructive to compare the relative pK_a values of the adenine derivatives with those obtained experimentally for the corresponding ATP derivatives **1**−**6** (Table 3). The predicted trend in pK_a values show excellent agreement with the experimental results, and the conclusions drawn regarding the substituent-dependent adenine basicity should also be valid for the corresponding ATP derivatives.

Discussion

The effect of the nature and position of adenine substituents on the acidity constant of ATP derivatives cannot be analyzed solely on the basis of structural considerations, such as inductive or resonance effect, H-bonding, steric effect, or hybridization. This is due to solvent effects that also contribute to the measured pK_a value. Specifically, the effects of ED or EW groups are much weakened in aqueous solutions and may even be reversed.

The most dramatic effect on N1 basicity was observed for 2-Cl-ATP, with more than 10,000-fold reduction of basicity compared with ATP. The pK_a value of −0.2 for 2-Cl-ATP is based on extrapolation (Tables 2 and 3)

(38) (a) Shcherbakova, I.; Elguero, J.; Katritzky, A. R. *Adv. Heterocycl. Chem.* **2000**, *77*, 51−113. (b) Brown, D. J. In *Comprehensive Heterocyclic Chemistry. The Structure, Reactions, Synthesis and Uses of Heterocyclic Compounds*. Katritzky, A. R., Rees, C. W., Eds.; Pergamon Press Ltd.: Oxford, 1984; Vol. 3, pp 67−68.

(39) Barone, V.; Cossi, M.; Tomasi, J. *J. Chem. Phys.* **1997**, *107*, 3210−3221.

because of the instability of nucleotides and inaccuracy of pH measurements at highly acidic solutions. This low value implies that the chloro substituent reduces considerably the electron density on the neighboring N1, as indeed reflected by ^{15}N chemical shift of N1 (Table 1). This result was supported by the calculated pK_a for 2-Cl-adenine, **16** (Table 5). The strong EW nature of Cl is clearly seen from the gas phase PA and GB (Table 5), and solvation does not significantly change the basicity of N1.

However, an EW group (Br) at C8 has only a minor effect on the nucleotide basicity, reducing the pK_a value of 8-Br-ATP to 3.83. 8-Br minimally destabilizes the protonated species as a result of the remote position, and this was confirmed by the calculated pK_a value for 8-Br-adenine. The gas-phase PA and GB of 8-Br- and 8-Cl-adenine, **17** and **21**, showed a slight decrease in proton affinity relative to adenine (Table 5). Thus, solvation slightly increases the basicity of 8-Br- and 8-Cl-adenine.

On the other hand, for 2-MeS-ATP, a pK_a value higher than that of ATP may be expected as a result of a mesomeric effect of the ED group. Yet, it is one pK_a unit lower than that of ATP. Apparently, the hydration effect reduces the expected basicity. This is probably due to a less favorable solvation of the protonated nucleotide as indicated by the quantum mechanical calculations. Analysis of the two terms comprising the ΔG^{prot}_{aq} of 2-MeS-adenine in eq 2, namely, ΔG^{prot}_{gas} and $\Delta\Delta G^{hyd}$, may give an insight into the origin of the shift in pK_a. The PA and the GB of 2-MeS-adenine, **13**, showed a clear ED effect compared to that of adenine (Table 5). However, it is found that the $\Delta\Delta G^{hyd}$ of 2-MeS-adenine is greater than that for adenine. This finding is due to the less favorable solvation of the N1-protonated 2-MeS-adenine compared to that of the N1-protonated adenine. The reduced solvation of the cationic 2-MeS-adenine is probably a result of the conjugation between the sulfur 3p (normal) lone pair and the adenine ring that delocalizes the positive charge. Moreover, the NH^+ moiety is not as solvent-accessible as in ATP because of the bulky thiomethyl group. Thus, the basicity of 2-MeS-adenine is lowered in a highly polar environment, although this does not mean that its inherent basicity (i.e., PA or GB) is lower than that of adenine.

When comparing 2-MeS-ATP with 2-$(CH_3)_3CCH_2$S-ATP a change of pK_a from 3.22 to 3.54 is observed. This change is due to the field contribution of the larger alkyl group, as observed from the calculated PA of 231.3 vs 228.9 kcal/mol for $(CH_3)_3CCH_2$S-adenine and 2-MeS-adenine, **14** and **13**, respectively.

In both 2-thioether-ATP derivatives investigated (**2**, **3**), a small extent of N7-protonation was observed in addition to N1 protonation, resulting in a mixed population of N1 and N7 singly protonated species. Both $N1H^+$ and $N7H^+$ species are formed at the same pH range, and the chemical shift of each of these nitrogens is equally effected by protonation. We therefore conclude, on the basis of $\Delta\delta$ values in Table 2, that for compounds **2** and **3** the ratio of equilibrating $N1H^+$ and $N7H^+$ species are 95:5, and 90:10, respectively. This conclusion is supported by our calculations that predict the N7 protonation to be less favorable by only 0.5 kcal/mol, with pK_a values of 3.25 for 2-MeS-adenine $N1H^+$ species and 2.85 for $N7H^+$ species. These findings indicate that both monoprotonated species may exist in solution.

Although 8-NH_2-ATP was not investigated in this study, it is of interest to compare the basicity of 8-NH_2-adenine to that of adenine. Interestingly, for 8-NH_2-adenine, **19**, N1 protonation is clearly favored in the gas phase. However, hydration makes the N7 protonation favored in the aqueous phase by 0.5 kcal/mol (Table 5) with pK_a values of 6.06 and 6.43 for $N1H^+$ and $N7H^+$ singly protonated species. Chattopadhyaya et al. demonstrated by ^{15}N NMR and semiempirical calculations that 8-amino and alkylamino substituents influence the properties of the resultant adenine ring system, including the relative basicity of N1 and N7 positions. The extent of N7 vs N1 protonation by TFA in DMSO was controlled by the nature of the substituent at the 8-amino group. For instance, 8-amino-adenosine was 66% N1 and 34% N7 protonated.[12a] This finding fits our results considering that DMSO is a less polar solvent than water.

A slight reduction in N1 basicity for N^6-Me-ATP, reflected in a pK_a value of 3.88, was rather unexpected on the basis of the high proton affinity of the corresponding adenine derivative, **15**, (228.8 kcal/mol). This PA value is due to a positive inductive effect of N^6-Me group. Yet, unfavorable hydration ($\Delta\Delta G^{solv}$ 216 kcal/mol) reverses the ED effect and the predicted pK_a value of N^6-Me-adenine, **15**, (3.71) vs adenine (3.95) is in a good agreement with the variations of the measured pK_a of ATP derivative **4** vs **1** (3.88 vs 4.16). The less favorable solvation may be attributed to increased delocalization of the protonated species, as in the case of the 2-thioether derivatives. Moreover, steric hindrance reduces the solvent-accessible surface of the $N1H^+$ group and restricts rotations of water molecules H-bonded to $N1H^+$, leading to an unfavorable entropy of solvation as seen in the $\Delta\Delta G^{hyd}$ term (Table 5). Indeed, N^6,N^6-diMe-adenosine is even less basic, with an experimental pK_a of 3.50.[12a] For the latter derivative, minor protonation was also observed at N3,[12a] although no protonation at this site was detected for N^6-Me-ATP.

Conclusions

In this study the acid/base character of a set of ATP prototypes was investigated using ^{15}N NMR spectroscopy, and the corresponding set of adenine bases was investigated by theoretical calculations. The prototypes studied are ATP analogues with ED or EW substituents at the C2-, C8-, or N^6-position of the adenine ring.

^{15}N NMR was utilized for the determination of acidity constants for ATP derivatives. The acidity constant obtained by ^{15}N NMR in H_2O solution for ATP is in good agreement with values obtained by various techniques. Furthermore, ^{15}N NMR measurements provided not only acidity constants for ATP derivatives **1**−**6** but also information on the protonation site(s) in the adenine ring and on the ratio between the different monoprotonated species existing in equilibrium. This is important information that cannot be easily obtained by most other titration techniques.

To supplement the experimental results, DFT calculations combined with PCM solvation calculations were performed, using PCM parameters that were fitted to reproduce experimental pK_a values of nitrogen heterocycles (PCM-pK_a). The quantum mechanical calculations (i.e., PA, GB, and $\Delta\Delta G^{hyd}$) provided sound explanations for the variations in pK_a of the ATP derivatives due to adenine ring substitutions. Therefore, this method is

proposed for the prediction of acidity and protonation site(s) of purine analogues that have not been synthesized or analyzed.

We found that substituents of different nature and position on the adenine ring in ATP derivatives **1**−**6** did not change the preferential protonation site, namely, the N1 position. For the 2-thioether-ATP derivatives we observed a mixed population of N1 and N7 monoprotonated species. The ratio between these species was 9:1 for compound **3**. This is a rather unexpected finding because of the remote position of the substituent.

Despite the different nature and position of substituents on the adenine moiety, for most evaluated ATP derivatives (**2**−**5**) the basicity of N1 was reduced by 0.4−1 pK_a units, relative to ATP. The most dramatic effect was observed for 2-Cl-ATP, where the acidity constant was ca. 10,000-fold lower.

Experimental Section

Apparatus and Measurements. NMR spectra were measured on a Bruker AC-200 instrument (200.2 and 80.3 MHz for ^{1}H and ^{31}P, respectively) or on a Bruker DPX-300 (300.1 and 75.5 MHz for ^{1}H and ^{13}C, respectively). ^{15}N NMR spectra were recorded on a Bruker DMX-600 instrument (60.8 MHz for ^{15}N) and measured with nitromethane (δ = 0 ppm) as an external standard. Negative chemical shifts are upfield from nitromethane. Determination of apparent pH values was made with a Hanna Instruments pH meter (HI 8521) equipped with an Orion microcombination pH electrode (9802) or Hanna instruments electrode (FC200). Neutral solutions of trisodium salts of the nucleotide derivatives at 0.9−1.2 M concentration range were titrated with dilute hydrochloric acid. ^{15}N NMR chemical shift of N1 was monitored as a function of the pH. A five-parameter sigmoid function was fitted to the data using SigmaPlot 2000 (SPSS, Inc.):

$$\delta = \delta_0 + \frac{a}{(1 + e^{-((\mathrm{pH}-\mathrm{pH}_0)/b)})^c} \qquad (7)$$

Full $\Delta\delta$ values for N1 (and other adenine nitrogens) were obtained from the fitted asymptotic values of the sigmoid titration curves (Table 3). The pK_a value, namely, the inflection point, was determined by the second derivative of the fitted sigmoid function. Ionic strength near the pK_a value is 2.8−3.3 M.

Materials. 8-Bromo-adenosine 5′-triphosphate and N^6-methyl-adenosine were purchased from Sigma Chemical Co. 2-Methylthio-adenosine was prepared according to a literature procedure.[41] 5′-Phosphorylated adenosine derivatives were prepared and purified according to our previous report.[14c]

2-[(2′,2′-Dimethyl-propyl)-thioether] Adenosine (8). A suspension of 2-thiol-adenosine[16] (700 mg, 3.34 mmol in 45 mL of MeOH) was dissolved in 0.25 M NaOH (10.3 mL) and stirred at room temperature for 1.5 h. The solvent was evaporated under high vacuum. The obtained thiolate sodium salt was then dissolved in dry DMF (40 mL), and 1-bromo-2, 2-dimethylpropyl (0.32 mL, 2.54 mmol) was added. The reaction mixture was stirred for 48 h at 80° C. TLC ($CHCl_3$/MeOH; 4:5) indicated that the entire starting material was consumed, and a new product was formed (R_f 0.33). The solvent was evaporated under reduced pressure, and the residue was separated on a silica gel column ($CHCl_3$/MeOH; 9:1). The product was obtained as a yellowish solid (445 mg, 52%). ^{1}H NMR (CD_3OD, 300 MHz) δ 8.17 (s, 1H, H-8), 5.93 (d, J = 6 Hz, 1H, H-1′), 4.73 (t, J = 5.5 Hz, 1H, H-2′), 4.34 (dd, J = 5, 3.5 Hz, 1H, H-3′), 4.14 (q, J = 3 Hz, 1H, H-4′), 3.89 (dd, J = 12.5, 3 Hz, 1H, H-5′), 3.75 (dd, J = 12.5, 3 Hz, 1H, H-5′), 3.24 (d, J = 1.5 Hz, 2H, SCH_2), 1.05 (s, 9H, CH_3). ^{13}C NMR (CD_3OD, 300 MHz) δ 167.2 (s, C-2), 156.7 (s, C-6), 151.2 (s, C-4), 140.6 (d, C-8), 121.1 (s, C-5), 90.7 (d, C-1′), 87.4 (d, C-4′), 75.3 (d, C-2′), 72.3 (d, C-3′), 63.3 (t, C-5′), 45.3 (t, SCH_2), 29.2 (q, CH_3). HRMS calcd for $C_{15}H_{24}N_5O_4S$ 370.1549, found 370.1562.

2-[(2′,2′-Dimethylpropyl)thioether] Adenosine 5′-Triphosphate (3). Obtained according to literature procedure[14c] in 71% yield. ^{1}H NMR (D_2O, 200 MHz) δ 8.21 (s, 1H, H-8), 6.01 (d, J = 4.5 Hz, 1H, H-1′), (H-2′ is hidden by water peak), 4.50 (t, J = 4.50 Hz, 1H, H-3′), 4.31 (br.s, 1H, H-4′), 4.20 (br.s, 2H, H-5′), 3.00 (s, 2H, SCH_2), 0.85 (s, 9H, CH_3). ^{31}P NMR (D_2O, 200 MHz) δ −6.67 (d), −10.26 (d), −20.87 (t). High-resolution FAB calcd for $C_{15}H_{25}N_5O_{13}P_3S$ 608.0382, found 608.0380.

2-Chloro-adenosine (11). A sealed ampule containing 2,6-dichloro-9β-(2′,3′,5′-tri-*O*-acetyl)-D-ribofuranosylpurine[17] (650 mg, 1.45 mmol) and 2 M NH_3/EtOH (60 mL) was heated to 100° C for 24 h. Stirring was continued for an additional 24 h at room temperature, and then the solvent was removed under reduced pressure. The residue was purified on silica gel chromatography (elution with $CHCl_3$/MeOH; 9:1). The product was obtained as a yellowish solid (322 mg, 73% yield). Spectral data is consistent with the literature.

Methods of Theoretical Calculations. Gas-phase calculations were performed using the B3LYP functional.[31] The geometries of all molecules were optimized with B3LYP and the 6-31G(d,p) basis set,[42] and the nature of the stationary points was investigated. In cases were local maxima were found, the structures were reoptimized with small geometry perturbations, stricter convergence criteria, more accurate grids, or accurate Hessian matrix. Zero-point energies and thermal corrections at 1 atm and 298 K were included. The computed zero-point energies were scaled by a factor of 0.9806, and the enthalpy and entropy contributions were scaled by 0.9989 and 1.0015, respectively.[43] Single-point calculations were then performed using B3LYP with the cc-pVTZ(-f) basis set augmented with diffuse functions on all atoms[34] (B3LYP/aug-cc-pVTZ(-f)//B3LYP/6-31G(d,p)). The cc-pVTZ(-f) basis set is the cc-pVTZ basis set of Dunning et al., but with the outmost polarization and diffuse functions deleted. In the case of bromine derivatives, the effective core potential LAVCP** basis set[44] was used for the bromine instead of 6-31G(d,p) and f-functions were kept in the cc-pVTZ basis set. For molecules containing anions, diffuse functions were added to the 6-31G-(d,p) basis set on all heavy atoms, both in the gas phase and in solution.

Solvent effects were included using PCM[29] with the B3LYP/6-31G(d,p) functional, and those for PCM-UAHF[39] with HF/6-31G(d,p). All compounds were optimized in aqueous solution using the ICOMP=2 keyword, while subsequent single point calculations used the more sophisticated ICOMP=4 option. Within the PCM approach, both the standard Pauling atomic radii with standard scaling factors were used (Gaussian 98 keywords: Pauling, AlphaH=1.0, Alpha=1.2) and the Pauling set with a set of scaling factors fitted to reproduce pK_a values (PCM-pK_a).

In the fitting process, the Pauling atomic radii set was used and the scaling factor was varied for each atom type (N, C, H, H(polar), S, Cl, Br) until the best fit with the experimental pK_a values was obtained. The scaling factor was initially defined as $f = 0.9 + 0.1n$ where n = 0, 1, 2, 3, 4, 5. After finding an optimal scaling factor for each atom, changes of ±0.05 were also tested. The optimal scaling factors are presented in Table 6, together with the atomic radii as defined in the Pauling set.

(40) (a) Hall, G. G. *Proc. R. Soc. London, Ser. A* **1951**, *205*, 541−552. (b) Roothaan, C. C. J. *Rev. Mod. Phys.* **1951**, *23*, 69−89.
(41) Macfarlane, D. E. *Methods Enzymol.* **1992**, *215*, 137−142.
(42) (a) Ditchfield, R.; Hehre, W. J.; Pople, J. A. *J. Chem. Phys.* **1971**, *54*, 724−728. (b) Hehre, W. J.; Ditchfield, R.; Pople, J. A. *J. Chem. Phys.* **1972**, *56*, 2257−2261. (c) Hariharan, P. C.; Pople, J. A. *Mol. Phys.* **1974**, *27*, 209−214. (d) Gordon, M. S. *Chem. Phys. Lett.* **1980**, *76*, 163−168. (e) Hariharan, P. C.; Pople, J. A. *Theo. Chem. Acta* **1973**, *28*, 213−222. (f) Francl, M. M.; Pietro, W. J.; Hehre, W. J.; Binkley, J. S.; Gordon, M. S.; DeFrees, D. J.; Pople, J. A. *J. Chem. Phys.* **1982**, *77*, 3654−3665.
(43) Scott, A. P.; Radom, L. *J. Phys. Chem.* **1996**, *100*, 16502−16513.
(44) (a) Hay, P. J.; Wadt, W. R. *J. Chem. Phys.* **1985**, *82*, 270−283. (b) Wadt, W. R.; Hay, P. J. *J. Chem. Phys.* **1985**, *82*, 284−298.

All calculations were performed using the Gaussian 98[45] and Jaguar 4.0[46] programs.

(45) Frisch, M. J.; Trucks, G. W.; Schlegel, H. B.; Scuseria, G. E.; Robb, M. A.; Cheeseman, J. R.; Zakrzewski, V. G.; Montgomery, J. A.; Stratmann, R. E.; Burant, J. C.; Dapprich, S.; Millam, J. M.; Daniels, A. D.; Kudin, K. N.; Strain, M. C.; Farkas, O.; Tomasi, J.; Barone, V.; Cossi, M.; Cammi, R.; Mennucci, B.; Pomelli, C.; Adamo, C.; Clifford, S.; Ochterski, J.; Petersson, G. A.; Ayala, P. Y.; Cui, Q.; Morokuma, K.; Malick, D. K.; Rabuck, A. D.; Raghavachari, K.; Foresman, J. B.; Cioslowski, J.; Ortiz, J. V.; Stefanov, B. B.; Liu, G.; Liashenko, A.; Piskorz, P.; Komaromi, I.; Gomperts, R.; Martin, R. L.; Fox, D. J.; Keith, T.; Al-Laham, M. A.; Peng, C. Y.; Nanayakkara, A.; Gonzalez, C.; Challacombe, M.; Gill, P. M. W.; Johnson, B. G.; Chen, W.; Wong, M. W.; Andres, J. L.; Head-Gordon, M.; Replogle, E. S.; Pople, J. A. *Gaussian 98*, Revision A.7; Gaussian, Inc.: Pittsburgh, PA, 1998.

Acknowledgment. This work was supported in part by the Marcus Center for Medicinal Chemistry. Dan T. Major thanks the Israeli Ministry of Science for financial support.

Supporting Information Available: Z-matrices with the computed total energies for adenine derivatives **12**−**22** and heterocycles **23**−**44**. This material is available free of charge via the Internet at http://pubs.acs.org.

JO0107554

(46) *Jaguar 4.0*; Schrödinger, Inc.: Pasadena, CA, 2000.